Author Manuscript

Author Manuscript

Author Manuscript

Author Manuscript

HHS Public Access

Author manuscript

Nature. Author manuscript; available in PMC 2017 April 30.

Published in final edited form as:

Nature. 2016 December 08; 540(7632): 280–283. doi:10.1038/nature20557.

Microcins mediate competition among Enterobacteriaceae in the inflamed gut

Martina Sassone-Corsi[1,2], **Sean-Paul Nuccio**[1,2], **Henry Liu**[1], **Dulcemaria Hernandez**[1], **Christine T. Vu**[1], **Amy A. Takahashi**[1], **Robert A. Edwards**[1,3], and **Manuela Raffatellu**[1,2,*]

[1]Department of Microbiology, University of California Irvine, Irvine, CA 92697, USA

[2]Institute for Immunology, University of California Irvine, Irvine, CA 92697, USA

[3]Department of Pathology and Laboratory Medicine, University of California, Irvine, CA 92697, USA

SUMMARY

The Enterobacteriaceae are Gram-negative bacteria and include commensal organisms as well as primary and opportunistic pathogens that are among the leading causes of morbidity and mortality worldwide. Although Enterobacteriaceae often comprise less than 1% of a healthy intestine's microbiota[1], some of these organisms can bloom in the inflamed gut[2–5]; indeed, expansion of enterobacteria is a hallmark of microbial imbalance known as "dysbiosis"[6]. Microcins are small secreted proteins that possess antimicrobial activity *in vitro*[7,8], but whose role *in vivo* has been unclear. Here we demonstrate that microcins enable the probiotic bacterium *Escherichia coli* Nissle 1917 (EcN) to limit expansion of competing Enterobacteriaceae (including pathogens and pathobionts) during intestinal inflammation. Microcin-producing EcN limited growth of competitors in the inflamed intestine, including commensal *E. coli*, adherent-invasive *E. coli*, and the related pathogen *Salmonella enterica*. Moreover, only therapeutic administration of the wild-type, microcin-producing EcN to mice previously infected with *S. enterica* substantially reduced intestinal colonization of the pathogen. Our work provides the first evidence that microcins mediate inter and intra-species competition among the Enterobacteriaceae in the inflamed gut. Moreover, we show that microcins can be narrow-spectrum therapeutics to inhibit enteric pathogens and reduce enterobacterial blooms.

Users may view, print, copy, and download text and data-mine the content in such documents, for the purposes of academic research, subject always to the full Conditions of use: http://www.nature.com/authors/editorial_policies/license.html#terms

*to whom correspondence should be addressed: Manuela Raffatellu, MD, Department of Microbiology and Molecular Genetics and Institute for Immunology, University of California, Irvine, Irvine, CA 92697, manuelar@uci.edu Fax: 949-824-8598 Tel: 949-824-0359.

AUTHOR CONTRIBUTIONS

M.S.-C. performed most bacterial growth assays, all animal experiments, and analyzed the results. S.-P.N. analyzed the microbiota data. R.A.E. scored histological sections. H.L., D.H., C.T.V., and A.A.T. assisted with mutant construction, bacterial growth assays, and animal experiments. M.S.-C. and M.R. were responsible for the overall study design. M.S.-C., S.-P.N., and M.R. wrote the manuscript.

CONFLICT OF INTEREST

The authors declare that they have no competing financial interests.

Author Manuscript Author Manuscript Author Manuscript Author Manuscript

TEXT

Broad-spectrum antibiotics are largely unsuccessful in treating enterobacterial gut infections. Efforts to identify novel therapeutics can be aided by identifying mechanisms beneficial microbes employ to mediate colonization resistance to pathogens[9,10]. Reports of microcin-producing Enterobacteriaceae in human stool led to hypotheses that microcins contribute gut microbial ecology[11]. Here we sought to identify an *in vivo* role for microcins by studying *Escherichia coli* Nissle 1917 (EcN)[12,13] and its interplay with related competitors in the gut. Similar to bacteriocins of Gram-positive bacteria, microcins can exhibit potent antibacterial activity *in vitro*[14–16]. In contrast to bacteriocins[15], a compelling *in vivo* role for microcins has not previously been demonstrated[17].

EcN's microcin gene cluster resides on Genomic Island I (Extended Data Fig. 1a and Supplementary Table 1) and encodes for microcin M (*mcmA*), microcin H47 (*mchB*), and their cognate immunity genes (*mcmI* and *mchI,* respectively). To understand whether EcN's microcins promote colonization of the healthy intestine, we intragastrically inoculated specific pathogen-free (SPF) mice with an equal mixture of a mouse commensal *E. coli* (cEc) strain[18] and either wild-type EcN or a mutant unable to secrete both microcins (EcN *mchDEF*)[14]. Although all strains poorly and transiently colonized the healthy intestine (enterobacteria typically colonize at low levels in this setting), cEc colonization was not significantly impacted by either wild-type EcN or EcN *mchDEF*, and cEc outcompeted both strains to a similar extent (Extended Data Fig. 1b–g).

To determine whether low colonization masked a microcin phenotype, we performed similar studies in germ-free mice and in streptomycin-treated SPF mice. We administered cEc alone or in competition with wild-type EcN, EcN *mchDEF,* or an EcN *mcmA mchB* mutant that lacks both microcin genes. All strains colonized the gut to high levels in these models, however cEc colonization was again unaffected by competition with EcN wild-type or microcin mutants (Fig. 1a,b). Moreover, there were no significant differences in colonization among EcN strains (Fig. 1c,d), and cEc outcompeted EcN wild-type and microcin mutants to a similar extent (Fig. 1e,f). Together, these results indicate EcN's microcins do not provide a competitive advantage under homeostatic conditions (Fig. 1g).

Prior work showed antibacterial activity for EcN's microcins in iron-limited media[14]. Moreover, a subset of microcins are post-translationally modified at the C-terminus with a siderophore moiety[19–21], and EcN's microcins are thought to be modified by a similar mechanism[14,21]. In response to iron starvation, commensals and pathogens synthesize and secrete siderophores to acquire this essential metal nutrient[22]. Bacterial uptake of iron-bound siderophores occurs via specific membrane receptors[14]. Microcins conjugated to siderophores are also synthesized during iron starvation, and can target non-immune bacteria *in vitro* through cognate siderophore receptors[14,16], a mechanism described as a 'Trojan horse' mode of action[7]. Incorporating these observations, we hypothesized that microcins contribute to competition among enterobacteria in the inflamed gut, where iron is limited[23].

We confirmed EcN's microcins (*mcmA*, *mchB*) are expressed in iron-limited media, and not in iron-rich media (Fig. 1h). To identify a role for microcins during intestinal inflammation,

Author Manuscript Author Manuscript Author Manuscript Author Manuscript

we utilized the dextran sulfate sodium (DSS)-treated mouse model of colitis (Fig. 2a). First, we intragastrically inoculated DSS-treated SPF mice with an equal mixture of cEc and wild-type EcN, EcN *mchDEF*, or EcN *mcmA mchB*. Although cEc initially outcompeted (~10-fold) wild-type EcN, both strains colonized the intestine equally well by day 5 post-inoculation. In contrast, cEc greatly outcompeted (up to 10,000-fold) the microcin mutants (Fig. 2b and Extended Data Fig. 2a). While intestinal colonization of cEc was similar when alone or in competition with wild-type EcN or a microcin mutant at day 1–3 post-inoculation, only wild-type EcN significantly reduced cEc colonization at later timepoints (Fig. 2c and Extended Data Fig. 2b,h). Consistent with this, *in vitro* killing of cEc was only observed in iron-limited media when competing with wild-type EcN, not the microcin mutants (Extended Data Fig. 3a–d). As the EcN microcin mutants still express cognate microcin immunity proteins, their competitive growth *in vitro* was not impaired (Extended Data Fig. 3c–g) until the immunity genes were deleted (Extended Data Fig. 3h,i). Nevertheless, gut colonization of microcin mutants was similarly reduced in competition with cEc (Fig. 2d and Extended Data Fig. 2c,*i*), whereas *trans*-complementation of EcN *mchDEF* restored colonization (Fig. 2b–d). As cEc was isolated from the murine gut, cEc is plausibly better adapted to growth in this environment than is EcN, a human isolate. Microcins thus give EcN a means by which to compete.

In contrast to competition with cEc, colonization of microcin mutants was not impaired in DSS-treated mice when strains were administered alone or in competition with wild-type EcN (Fig. 3a–c and Extended Data Fig. 4a–d). Microcin mutants exhibited a 5–10-fold advantage over wild-type EcN at day 5 post-inoculation (Fig. 3c), which may result from the mutants still being immune to microcins and not expending energy on microcin production; relatedly, wild-type EcN rescued colonization of microcin mutants when co-administered with cEc in DSS-treated mice (Extended Data Fig. 4e–h). Microcin mutants are thus not intrinsically attenuated. Moreover, our findings indicate that microcins enable EcN to limit expansion of a related commensal in the inflamed gut (Extended Data Fig. 2d–g), where Enterobacteriaceae thrive but also compete with each other for space and limited nutrients (niche competition).

We next tested whether iron supplementation during colitis inhibited microcin activity. Mice fed an iron-rich diet three weeks prior to and during DSS treatment developed colitis, yet wild-type EcN did not reduce colonization of cEc. Instead, both EcN wild-type and EcN *mchDEF* were outcompeted by cEc and exhibited similar levels of gut colonization (Extended Data Fig. 5a–e). Thus, if iron is supplemented, microcins do not limit expansion of a competitor in the inflamed gut, likely because microcins, siderophores and siderophore receptors (i.e., microcin receptors) are only expressed during iron starvation[14,23]. These observations also suggest that, in contrast to broad-spectrum antibiotics, siderophore-linked microcins would have a limited effect on the gut microbiota as they target strains that acquire those siderophores.

As microcins mediated competition between EcN and cEc in the DSS-colitis model, we analyzed the intestinal microbiota in this setting. DSS treatment reduced the gut microbiota's diversity (Extended Data Fig. 5f), and subsequent administration of wild-type EcN or EcN *mchDEF* yielded similar shifts in microbial communities (Extended Data Fig.

Author Manuscript Author Manuscript Author Manuscript Author Manuscript

5f,g and Supplementary Table 2). These results indicate that, at least in our DSS-treated mice, EcN's microcins did not substantially change the gut microbiota, which is consistent with their predicted narrow spectrum.

In addition to some commensal Enterobacteriaceae, some enterobacterial pathogens thrive in the inflamed gut[3]. We therefore investigated microcins' activity against the diarrheal pathogen *Salmonella enterica* serovar Typhimurium (STm). We first established that wild-type EcN, but not EcN *mchDEF* or EcN *mcmA mchB*, only killed STm in iron-limited media (Extended Data Fig. 6a–e). When streptomycin-treated mice (*Salmonella* colitis model) were co-administered STm and either wild-type EcN or EcN *mchDEF*, only wild-type EcN outcompeted STm beyond day 4 post-infection (Fig. 3d,e). Although all strains initially colonized the gut to similar levels, reduction of STm colonization was significantly enhanced by microcin-producing EcN (Fig. 3f). By day 7, wild-type EcN and EcN *mchDEF* had similarly reduced STm colonization, likely because EcN has other mechanisms to outcompete STm, including a greater ability to acquire iron[23]. Nevertheless, in agreement with our cEc results (Fig. 2a–d), gut colonization of EcN *mchDEF* was drastically reduced in competition with STm 7 days after co-administration (Fig. 3g). Moreover, wild-type EcN's competitive advantage over STm was again only observed during intestinal inflammation **(**Extended Data Fig. 7a,b). Relatedly, wild-type EcN and EcN *mchDEF* showed similar levels of intestinal colonization and no competitive advantages when competed with STm *invA spiB*, a mutant in both type-three secretion systems that is unable to trigger gut inflammation as it cannot invade the intestinal epithelium or replicate intracellularly (Extended Data Fig. 7c–e).

Consistent with our STm and cEc results, microcins impaired growth of adherent invasive *E. coli* (AIEC), a pathobiont frequently isolated from Crohn's disease patients. Wild-type EcN, but not EcN *mchDEF*, was able to reduce AIEC growth *in vitro* (Extended Data Fig. 6f–i) and in the DSS-colitis model (Extended Data Fig. 8). Although AIEC and wild-type EcN colonized the inflamed gut to similar levels, AIEC significantly outcompeted EcN *mchDEF* in this environment (Extended Data Fig. 8). Collectively, our data indicate that EcN produces microcins to limit growth of competing enterics in the inflamed gut.

We next investigated whether microcins could therapeutically treat an active enterobacterial infection, administering EcN wild-type or EcN *mchDEF* to mice previously infected with STm (Fig. 4a). Mice receiving wild-type EcN at days 2 and 5 post-STm infection showed substantially reduced STm gut colonization (average 1,300-fold; up to 100,000-fold), inflammation and weight loss (Fig. 4b–d and Extended Data Fig. 9). This phenotype largely depended on microcins, as EcN *mchDEF* only minimally reduced STm intestinal burden (~17-fold), and did not reduce inflammation or weight loss (Fig. 4b–d and Extended Data Fig. 9). To better understand the therapeutic phenotype, we assayed each microcin's antibacterial activity.

While microcins M and H47 showed antibacterial activity against AIEC, only M was effective against STm and cEc (Extended Data Fig. 10a–c); the H47-resistance mechanism is unknown as neither strain carries *mchI*. Accordingly, STm engineered to express *mchI* (STm pMchI) was not rescued in competition with wild-type EcN, whereas STm pMcmI was

Author Manuscript Author Manuscript Author Manuscript Author Manuscript

rescued (Extended Data Fig. 10d,e). Strikingly, therapeutic administration of EcN only minimally impaired colonization of the microcin-resistant STm pMcmI (Fig. 4b and Extended Data Fig. 9). Furthermore, inflammation, weight loss and STm colonization were comparable when either EcN *mchDEF* or STm pMcmI were used in the therapeutic experiment (Fig. 4b–d and Extended Data Fig. 9).

Altogether, we provide the first *in vivo* evidence that microcins mediate competition among Enterobacteriaceae in the inflamed gut. We show that the probiotic bacterium EcN employs microcins to compete with related species, colonize the inflamed gut, and therapeutically displace an enteric pathogen from its niche. EcN's microcins target microbes expressing particular siderophore receptors, and do not severely impact the microbiota. Although siderophore receptor mutants are resistant ([14] and Extended Data Fig. 10f–h), they are attenuated in the inflamed intestine[24] and thus unlikely to be selected for. As microcins were particularly effective during therapeutic EcN administration to pathogen-infected, inflamed mice, these or similar compounds (e.g., siderophore-conjugated antibiotics[25]) could conceivably be utilized as a targeted strategy to treat enterobacterial colitis.

METHODS

Bacterial Strains, culture conditions and chemicals

Strains of the probiotic *Escherichia coli* Nissle 1917 (EcN; Mutaflor, DSM 6601), the mouse commensal *Escherichia coli* (cEc), the adherent invasive *E. coli* (AIEC), and the pathogen *Salmonella enterica* serovar Typhimurium (STm) utilized in this study are listed in Supplementary Table 3. All plasmids used in this study are listed in Supplementary Table 4. EcN was kindly provided by Ardeypharm Gmb, Herdecke, Germany. The commensal *E. coli* strain was isolated from mice in our vivarium and does not appear to encode for known antibacterial exoproducts. The AIEC strain is a human isolate from a patient with Crohn's disease (isolate NRG857c O83:H1)[26] and was kindly provided by Dr. Alfredo Torres. IR715 is a fully virulent, nalidixic acid-resistant derivative of STm wild-type isolate ATCC 14028, and does not encode for known antibacterial exoproducts. All strains were routinely grown aerobically in Luria-Bertani (LB) broth (10 g/L tryptone, 5 g/L yeast extract, 10 g/L NaCl) or on LB agar plates at 37 °C. When indicated, antibiotics were added to the media at the following concentrations: 0.03 mg/mL chloramphenicol (Cm); 0.1 mg/mL carbenicillin (Carb); 0.05 mg/mL kanamycin (Kan); 0.01 mg/mL tetracycline (Tet). For animal infections or bacterial administration, all strains were grown in LB media aerobically at 37 °C overnight. For *in vitro* growth assays, strains were grown in iron-limiting conditions (Nutrient Broth supplemented with 0.2 mM 2,2′-dipyridyl dissolved in ethanol; Sigma) aerobically at 37 °C overnight. Restrictions enzymes and Phusion High Fidelity DNA Polymerase were purchased from New England Biolabs. Oligonucleotides were synthesized by Fisher Scientific and are listed in Supplementary Tables 5 and 6.

Generation of bacterial mutants

Mutants in EcN and STm were constructed using the lambda red recombinase system[27]. Briefly, primers (Supplementary Table 5) homologous to sequences flanking the 5′ and 3′ ends of the target regions were designed (H1 and H2 primers, respectively; Supplementary

Author Manuscript Author Manuscript Author Manuscript Author Manuscript

Table 5) and were used to replace the selected genes with a chloramphenicol (derived from pKD3), kanamycin (derived from pKD4), or tetracycline resistance cassettes (Supplementary Table 4). Strain names for the mutants are listed in Supplementary Table 3. To confirm integration of the resistance cassette and deletion of the target, mutant strains and wild-type controls were each assayed utilizing three PCR amplifications (5′ end, 3′ end, deleted target) to validate mutations. Primers (Supplementary Table 5) that flank the target sequence were used in conjunction with a common test primer (C1, C2, K1, K2 or primers for the *tetRA* cassette) to test for both new junction fragments.

Complementation studies

The *mchDEF* region was amplified from EcN genomic DNA using primers listed in Supplementary Table 5. A region of 4148 bp was amplified to ensure all regulatory elements were included. The PCR fragment was cloned into plasmid pCR-XL-TOPO using Invitrogen's Zero Blunt TOPO PCR Cloning Kit's provided protocol, subcloned into the multiple cloning site of low copy plasmid pWSK29, and confirmed by Sanger sequencing (Eton Bioscience). The *mchDEF mcmI* and *mchDEF mchI* constructs were amplified from EcN genomic DNA using primers listed in Supplementary Table 5. PCR fragments of 4321 bp (*mchDEFmcmI*), 4000 bp (*mchDEF*) and 400 bp (*mchI*) were directly assembled with plasmid pWKS30 using the Gibson assembly method.

In vitro growth assays

The role of EcN's microcins against cEc, AIEC and STm was tested by *in vitro* competitive growth assay in iron-rich and iron-limiting conditions. Strains were grown in Nutrient Broth supplemented with 0.2mM 2,2′-dipyridyl (Sigma) aerobically at 37 °C overnight. Approximately 5×10^3 CFU/mL from an overnight culture were inoculated into 0.1 mL of tissue culture medium (DMEM/F12 with 10% fetal bovine serum (FBS); Invitrogen), as previously described[23,24]. When indicated, media was prepared with 1 μM ferric iron citrate (Sigma). Wild-type EcN or EcN mutants were inoculated in competition with wild-type STm, STm mutants, cEc, or AIEC. CFUs of each strain were enumerated by plating serial dilutions at 0, 5, 8, 11 and (for some assays) 16 h post-inoculation.

Mice

The Institutional Animal Care and Use Committee at the University of California, Irvine approved all mouse experiments. Eight to ten-week-old male and female C57BL/6 NRAMP1+ mice were bred and housed in our vivarium. For some experiments, mice were purchased from Jackson laboratory and upon arrival allowed to acclimate to the new environment for at least one week prior to the start of an experiment. All mice were housed under specific pathogen-free conditions. Mice were fed an irradiated 2920X Teklad diet (Envigo). For one experimental procedure mice were fed an irradiated iron rich diet (1% Diet $FeSO_4$ 2020, Teklad TD 160234; Envigo). Culturing feces on MacConkey agar indicated that culturable enterobacteria were absent from our mice. Five to ten mice were used per experimental group, as indicated by the number of symbols in each figure panel. Group sizes were based on previous studies that detected a 10-fold difference with statistical significance. For one experiment, 10 week-old Swiss Webster germ-free mice were used. Swiss Webster germ-free mice were maintained in sterile isolators and were fed a double-

Author Manuscript Author Manuscript Author Manuscript Author Manuscript

irradiated diet (Purina 5066, Charles River Rodent 18% Vac Pac). 3 mice per experimental group were used for this experimental procedure (see figure panels). Mice were randomly grouped in cages of a maximum five animals per cage. Similar numbers of male and female mice were used in each experimental group. No blinding was performed, with the exception of histopathology.

Dextran sulfate sodium-induced colitis mouse model

Drinking water was replaced with either filter-sterilized water (mock-treatment) or with a filter-sterilized solution of 4% (w/v) dextran sulfate sodium (DSS; relative molecular mass 36,000–50,000; MP Biomedicals, Santa Ana) in water as indicated. For DSS- treated mice, 3 days prior to the end of the experiment, drinking water was switched for 24h to filter-sterilized water. Drinking water was then replaced with either filter-sterilized water (mock-treatment) or with a filter-sterilized solution of 2% (w/v) DSS. 4 days after the start of DSS treatment, animals were orally inoculated with a 1:1 ratio of 5×10^8 CFU of wild-type EcN and mutants in competition with cEc or AIEC strains (resuspended in 0.1 mL LB broth). Fecal material was collected each day after bacterial administration, resuspended in sterile PBS and the bacterial load was determined by plating serial 10-fold dilutions on selective agar plates. Animals were euthanized 5 days after inoculation. Cecal tissue was collected then flash frozen in liquid nitrogen and stored at −80 °C for later isolation of mRNA and protein. The cecal tip was fixed in 10% formalin for histopathology. Fecal material and cecal content were harvested in sterile PBS and the bacterial load for the *E. coli* strains was determined by plating serial 10-fold dilutions on selective agar plates. At some timepoints, a mouse did not produce fecal material, hence an n is displayed for a given timepoint that is less than the experiment's indicated n for that group. To differentiate EcN from other *E. coli* strains in biological samples, the strains were differentially marked with the low-copy number pACYomega (Cm) or pHP45omega (Carb) (Supplementary Table 4), and markers were swapped in some experiments. Plasmids were stably maintained throughout the infection and similar colonies were counted in other differential media such as MacConkey agar (not shown). When noted, the ratio of two strains in the feces and cecal content was calculated by dividing the output ratio (EcN CFU/cEc or AIEC CFU) by the input ratio (EcN CFU/cEc or AIEC CFU). The competitive index was calculated for isogenic strains by dividing the output ration (EcN wild-type CFU/mutant CFU) by the input ration (EcN wild-type CFU/mutant CFU).

Salmonella Typhimurium-induced colitis

C57BL/6 NRAMP1+ mice were treated with streptomycin (100 μL of a 200 mg/mL solution in sterile water) one day prior to infection. The following day, mice were orally inoculated with 1×10^9 CFU of STm (resuspended in 0.1 mL LB broth) or with a 1:1 ratio of 5×10^8 CFU each of STm and wild-type EcN, or EcN *mchDEF* strain for competitive colonization experiments. For therapeutic administration of EcN after STm infection, C57BL/6 NRAMP1+ mice were treated with streptomycin (100 μL of a 200 mg/mL solution in sterile water) one day prior to STm infection. The following day, mice were orally inoculated with 1×10^9 CFU of STm. At days 2 and 5 after STm infection, mice were either mock-treated or treated with 1×10^9 CFU of wild-type EcN or EcN *mchDEF*. Fecal material was collected each day after bacterial administration, resuspended in sterile PBS, then bacterial load for

Author Manuscript Author Manuscript Author Manuscript Author Manuscript

STm and EcN strains was determined by plating serial 10-fold dilutions on selective agar plates. At some timepoints, a mouse did not produce fecal material, hence an n is displayed for a given timepoint that is less than the experiment's indicated n for that group. At day 7 post-infection, mice were euthanized and a portion of the cecum was flash frozen in liquid nitrogen then stored at −80 °C for later isolation of mRNA and protein. The cecal tip was fixed in 10% formalin for histopathology. Bacteria were enumerated in the fecal content by plating serial 10-fold dilutions on LB agar plates containing appropriate antibiotics. To selectively identify STm from EcN strain in the fecal content, strains were differentially marked with the low-copy number pACYomega (Cm) or pHP45omega (Carb) plasmids. Plasmids were stably maintained throughout the infection and similar colonies were counted in other differential media such as MacConkey agar (not shown). When noted, ratio of two strains was calculated by dividing the output ratio (EcN CFU/STm CFU) by the input ratio (EcN CFU/STm CFU).

Extraction of bacterial DNA from fecal samples

Fecal samples were collected prior to DSS treatment (day -4), at day 4 post-DSS treatment (day 0; before inoculation of bacteria) and at day 5 post-administration of commensal *E. coli* in competition with wild-type EcN or EcN *mchDEF*. Feces were snap frozen in liquid nitrogen, then DNA was later extracted using the QIAamp DNA Stool Kit (Qiagen) according to the manufacturer's instructions with modifications as previously described[18]. Because DSS interferes with PCR, we used the following procedure (developed by Dr. Wenhan Zhu and Dr. Sebastian Winter, UT Southwestern) to eliminate DSS from samples. Samples were eluted in 200 μl of ultrapure water and combined with 80 mg of KCl followed by vortexing for 2 min. The mixture was then incubated on ice for 30 min and centrifuged at 16,800 × g at 4 °C for 30 min. The supernatant was then transferred to a new tube and 1/10 volume of 3 M NaAc (pH 5.2) was added. 2.5 mL of pure ethanol was then added to the mixture, vortexed and centrifuged at 16,800 × g at 4 °C for 30 min. The supernatant was removed and 1 mL of 70% Ethanol was added to the pellet, vortexed and centrifuged at 16,800 × g for 5 min at RT. This wash step was repeated 3–4 times. The pellet was then air dried at 55 °C and resuspended in 30 μl of ultra-pure water.

Analysis of microbiota

DNA extracted from fecal samples was amplified by a two-step PCR enrichment of 16S rDNA (V4 region) with primers 515F and 806R modified by addition of barcodes for multiplexing, then sequenced on an Illumina MiSeq system (UC Davis HMSB Facility). Sequences were processed and analyzed by employing the QIIME pipeline v1.9.1[28] with default settings, except as noted. In brief: paired-end sequences were joined, quality filtered, reverse complemented, and chimera filtered (usearch61 option; RDP gold database); operational taxonomic units (OTUs) were picked (usearch61 option; enable_rev_strand_match True) at 97% similarity; taxonomy was assigned (confidence 0.8) with the RDP classifier. Greengenes database v13_8 was utilized in the open-reference OTU picking workflow.

Author Manuscript Author Manuscript Author Manuscript Author Manuscript

Bacterial RNA extraction

A bacterial RNA mini kit (Bio-Rad Aurum Total) was used to extract RNA from bacterial cultures. EcN strains were grown in Nutrient Broth supplemented with 0.2 mM 2,2′-dipyridyl aerobically at 37 °C overnight. Approximately 10^4 CFU/mL from an overnight culture were inoculated into 5 mL of tissue culture medium (DMEM/F12 plus 10% fetal bovine serum, Invitrogen), as previously described[23,24]. When indicated, iron citrate was added to the media at a final concentration of 1μM. At 7 h post-inoculation, 2×10^9 CFU were used to extract RNA. An additional DNAse treatment (Ambion) was done prior to the generation of cDNA with reverse transcription reagents (Roche).

Quantitative Real-Time PCR

For analysis of gene expression by quantitative real-time PCR, total RNA was extracted from cecal tissue with TRI Reagent (Molecular Research Center; Cincinnati, OH). RNA from DSS-treated mice was further purified using the Dynabeads mRNA DIRECT Purification Kit (Life Technologies) according to manufacturer recommendations. Reverse transcription reagents (Roche) were employed to generate cDNA from all RNA samples. Real-time PCR was performed using SYBR Green (Roche, Indianapolis, IN) and the Roche Lightcycler 480 Instrument II system (Roche, Indianapolis, IN). Data were analyzed using the comparative delta-delta-Ct method. Target gene transcription of each tissue sample was normalized to the respective levels of *Actb* mRNA (β-actin). For qPCR analysis of bacterial transcripts, transcription of *mcmA* and *mchB* was normalized to bacterial *gapA* mRNA levels. Data represents at least three independent experiments. DNA contamination was less than 1% for all bacterial amplicons, as determined by separate mock reactions lacking reverse transcriptase. All primers used are listed in Supplementary Table 6.

Histopathology analysis

Tissue samples were fixed in 10% formalin, processed according to standard procedures for paraffin embedding, sectioned at 5 mm, and stained with hematoxylin and eosin. The pathology score of cecal samples was determined by blinded examination of cecal sections from a board-certified pathologist using previously published methods[18]. Each section was evaluated for the presence of neutrophils, mononuclear infiltrate, submucosal edema, surface erosions, inflammatory exudates, and cryptitis. Inflammatory changes were scored from 0 to 4 according to the following scale: 0 = none; 1 = low; 2 = moderate; 3 = high; 4 = extreme. The inflammation score was calculated by adding up all scores obtained for each parameter and interpreted as follows 0–2 = within normal limit; 3–5 = mild; 6–8 = moderate; 8+ = severe.

Statistical analysis of data

Prism 6 and 7 software (Graphpad) was used for statistical analysis. Bacterial growth curves were analyzed by unpaired Student's *t* test. To compare bacterial CFUs in feces and cecal content, mRNA expression, and eubacterial taxa present at greater than 0.5% relative abundance in at least one sample, we applied a non-parametric Mann-Whitney-Wilcoxon test. We chose this test because it can be applied to data with normal or unknown

Author Manuscript Author Manuscript Author Manuscript Author Manuscript

distribution. *P*-values for all statistical comparisons presented in the main and extended data figures are available in Supplementary Table 7.

Data availability

The data that support the findings of this study are available from the corresponding author upon request. Fecal microbiota 16S rDNA sequencing data were deposited in the European Nucleotide Archive under accession PRJEB15700.

Extended Data

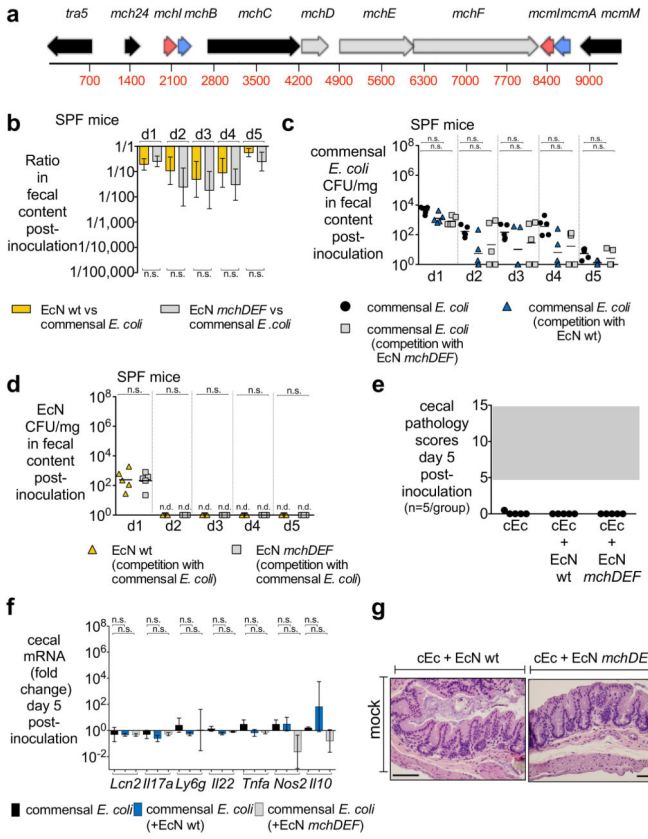

Extended Data Figure 1. *E. coli* Nissle wild-type and microcin mutant (*mchDEF*) gut colonization in competition with commensal *E. coli* in the absence of intestinal inflammation

a, Illustration of the microcin gene cluster in EcN**. b–g**, Intragastric inoculation of SPF mice with cEc alone or in competition with wild-type EcN or EcN *mchDEF* at a 1:1 ratio. **b**, Ratio (EcN over cEc) in fecal content at days 1–5 post-inoculation (n = 5/group). **c,d**, CFU/mg of (**c**) cEc or (d) wild-type EcN or EcN *mchDEF* in fecal content at days 1–5 post-inoculation, when cEc was administered alone or in competition as indicated. **e,f**, Cecal (e) histopathology scores or (**f**) gene expression (data are expressed as fold change over mock-treated mice) at day 5 post-inoculation for panels **b–d** (n = 5/group). **g**, H&E-stained sections from representative animals at day 5 post-inoculation; scale bar = 100 μm. **b**,**f**, Bars = geometric mean ± s.e.m. **c–e**, Individual symbol = mouse. **c,d**, Bars = geometric mean. **e**, Bars = mean. n.s., not significant.

Author Manuscript Author Manuscript Author Manuscript Author Manuscript

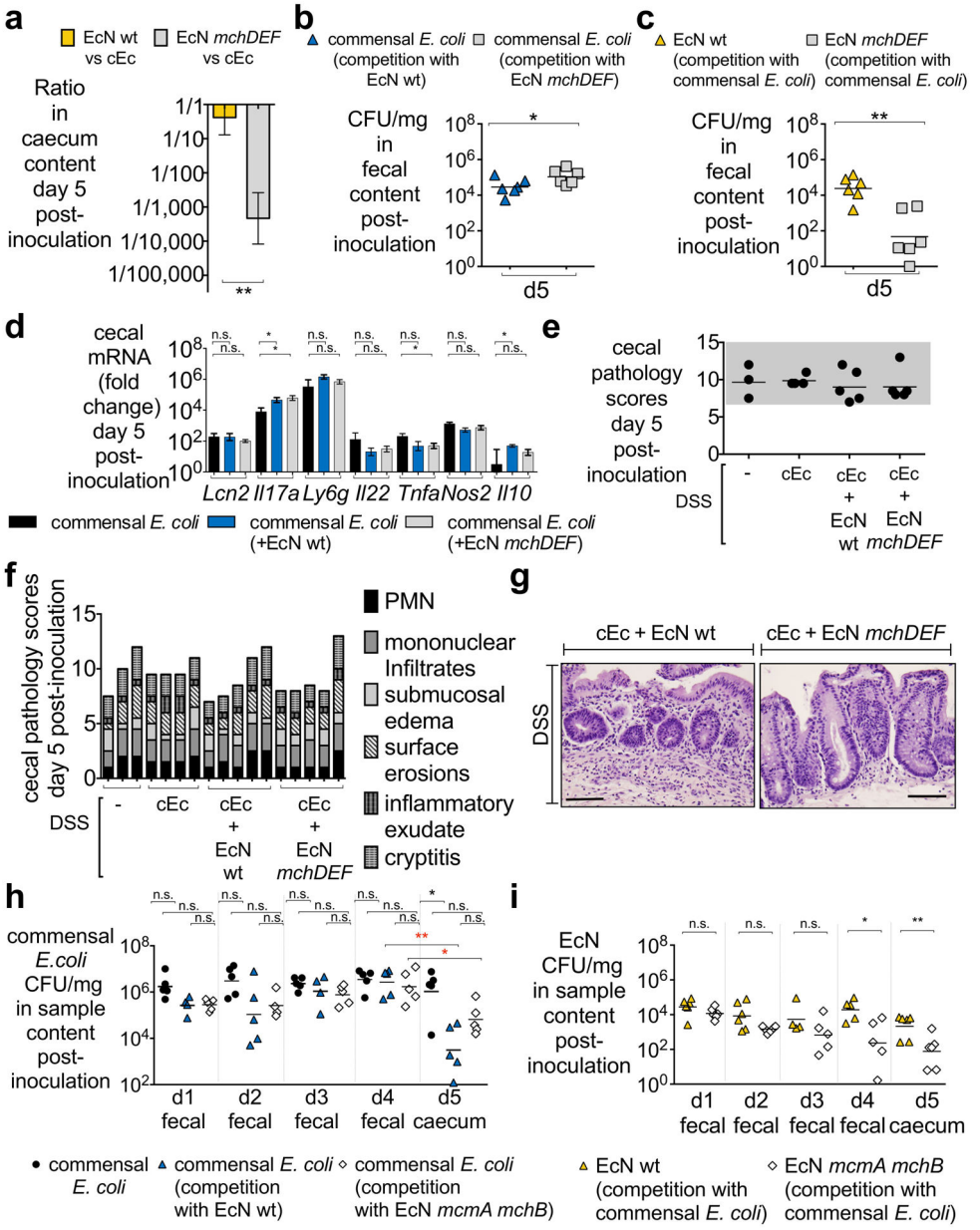

Extended Data Figure 2. Colonization and histopathology of *E. coli* Nissle wild-type and microcin mutants (*mchDEF* and *mcmA mchB*) in competition with commensal *E. coli*, in mice with DSS-mediated colitis

a–i, Experimental design as in Fig. 2a with SPF mice. **a**, Ratio (EcN over cEc) in cecal content at day 5 post-intragastric inoculation (n = 6/group). **b,c**, CFU/mg of (**b**) cEc or (**c**) wild-type EcN or EcN *mchDEF* in fecal content at day 5 post-inoculation when in competition as indicated (n = 6/group). **d,e**, Cecal (**d**) gene expression (n = 5/group) data are presented as fold change over mock-treated mice) or (**e**) histopathology scores at day 5 post-inoculation from mice shown in panels **b,c** and Fig. 2b–d (DSS only, n = 3; all others, n = 5); scale bar = 100 μm. **f**, Detailed histopathology scoring of panel **e** mice. **g**, H&E-stained sections from representative animals at day 5 post-inoculation. **h,i**, CFU/mg of (**h**) cEc or (**i**)

wild-type EcN or EcN *mcmA mchB* in sample content at days 1–5 post-intragastric inoculation when cEc was administered alone or in competition as indicated (n = 5/group). **a**,**d**, Bars = geometric mean ± s.e.m. **b**,**c**,**e**,**h**,**i**, Individual symbol = mouse. **b,c,h,i**, Bars = geometric mean. **e**, Bars = mean. **P*<0.05, ***P*<0.01; n.s., not significant.

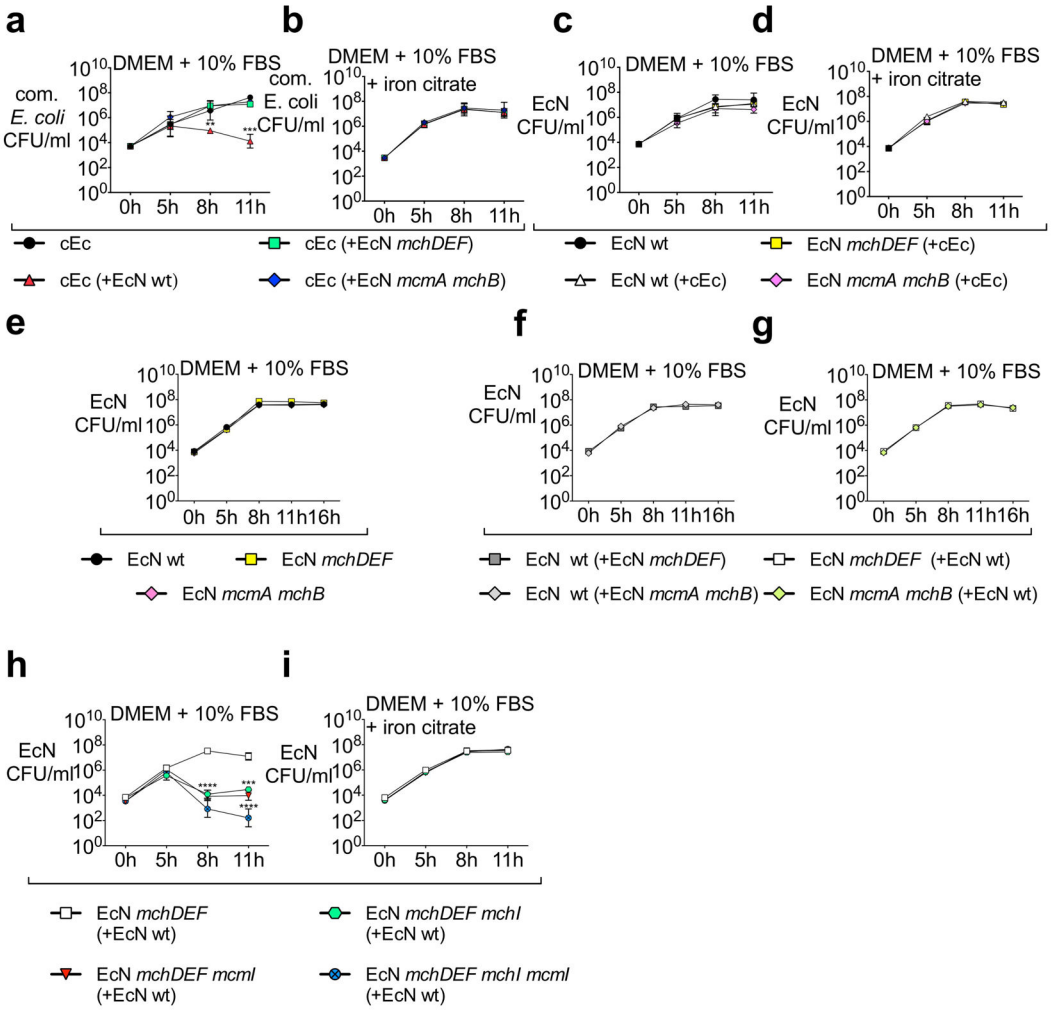

Extended Data Figure 3. *In vitro* growth curves of *E. coli* Nissle and microcin mutants when grown alone or in competition with EcN mutants or commensal *E. coli*

a–i, Strains were grown overnight in Nutrient Broth + 0.2 mM 2,2'-dipyridyl. Growth assays were performed in iron-limiting conditions (DMEM/F12 + 10% FBS) or in media supplemented with 1 μM iron citrate. Timepoints at 0, 5, 8 and 11 hours post-inoculation were collected. **a**,**b**, cEc CFU/mL when grown alone or in competition with wild-type or mutant EcN in (**a**) iron-limiting conditions or in (**b**) media supplemented with 1 μM iron citrate. **c**,**d**, CFU/mL of wild-type or mutant EcN when grown alone or in competition with cEc in (**c**) iron-limiting conditions or in (**d**) media supplemented with 1 μM iron citrate. **e–g**, Under iron-limiting conditions, CFU/mL of (**e**) wild-type or mutant EcN when grown alone, or of (f) wild-type EcN or (g) EcN *mchDEF* or EcN *mcmA mchB* when grown competitively as indicated**. h**,**i**, CFU/mL of the indicated EcN mutants (immunity gene(s)

Author Manuscript Author Manuscript Author Manuscript Author Manuscript

Author Manuscript Author Manuscript Author Manuscript Author Manuscript

and/or *mchDEF*) grown in competition with wild-type EcN in (**h**) iron-limiting conditions or in (**i**) media supplemented with 1 μM iron citrate. **a–i**, Symbols = geometric mean (three independent experiments) ± s.e.m. ***P*<0.01, ****P*<0.001, *****P*<0.0001.

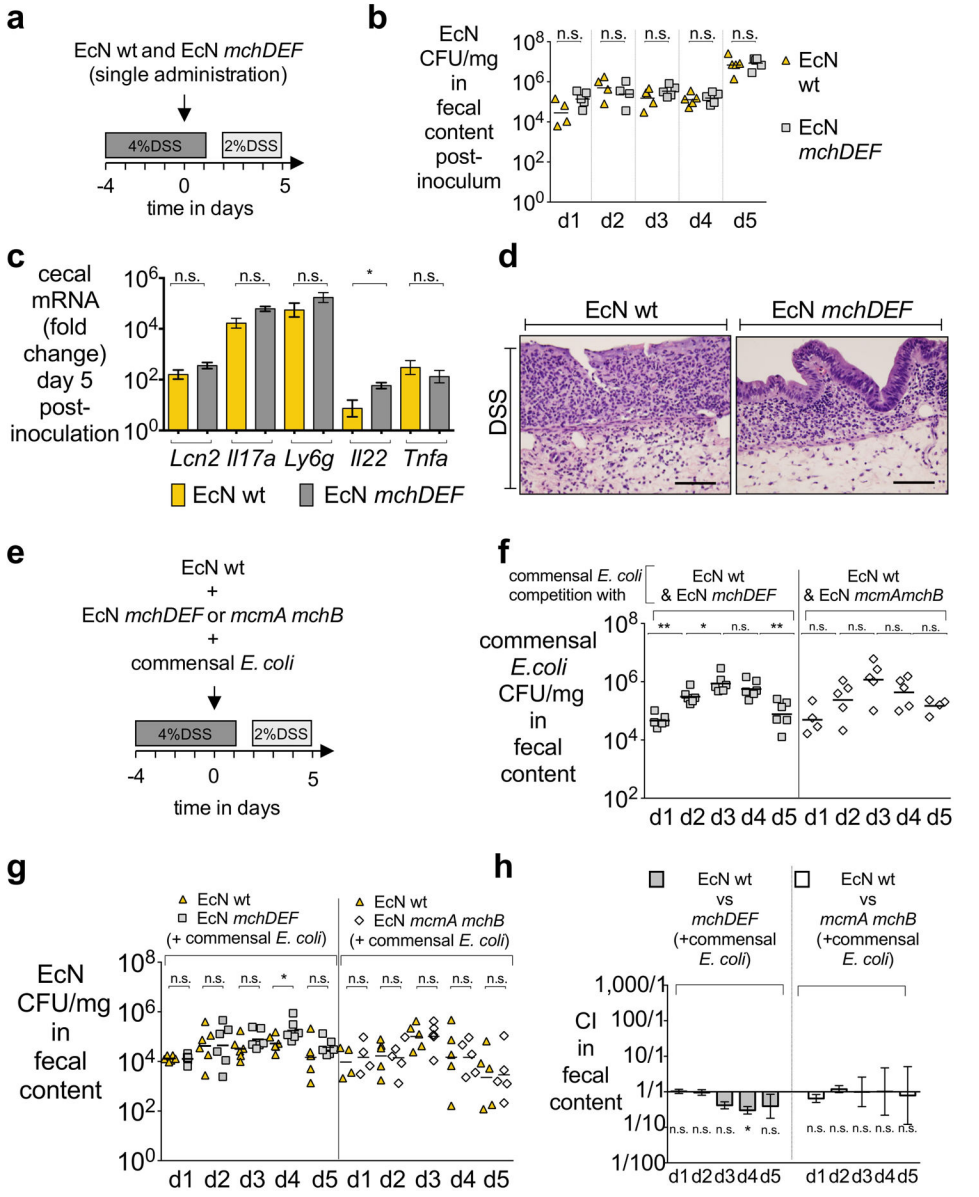

Extended Data Figure 4. Gut colonization of *E. coli* Nissle wild-type and microcin mutants in the DSS-colitis model

a, Experimental design for **b**-**d** with SPF mice. **b**, CFU/mg of wild-type EcN or EcN *mchDEF* in fecal content at days 1–5 post-intragastric inoculation (n = 5/group). **c,d**, Cecal (**c**) gene expression (n = 5/group; data are expressed as fold change over mock-treated mice) or (**d**) H&E-stained sections (representative) from panel **b** mice at day 5 post-inoculation; scale bar = 100 μm. **e**, Triple co-administration design for **f–h** with SPF mice. **f,g**, CFU/mg of (**f**) cEc or (**g**) indicated EcN strain in fecal content at days 1–5 post-intragastric

Author Manuscript Author Manuscript Author Manuscript Author Manuscript

inoculation with cEc, wild-type EcN and the indicated EcN mutant (n = 5/group). **h**, Competitive index (CI; EcN wild-type over mutant) for EcN data presented in panel **g** (n = 5/group). **b,f,g**, Individual symbol = mouse; bars = geometric mean. **c,h,** bars = geometric mean ± s.e.m. **P*<0.05, ***P*<0.01; n.s., not significant.

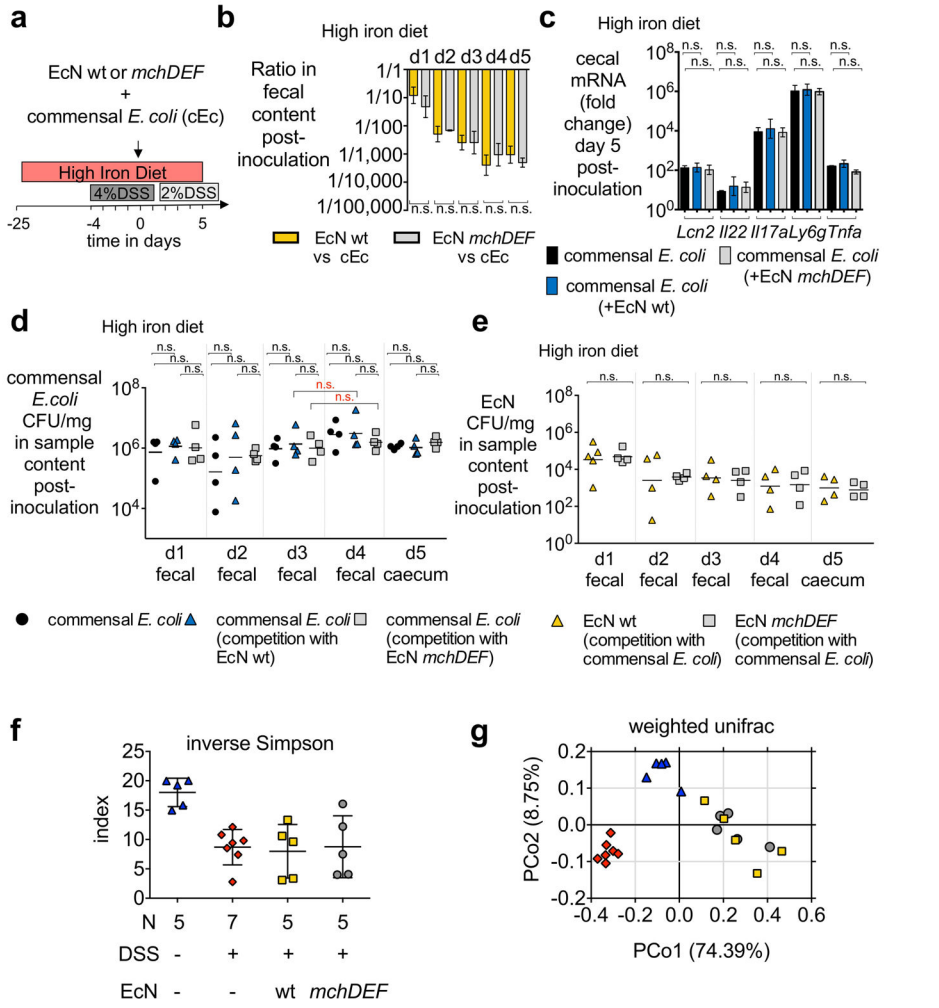

Extended Data Figure 5. Impact of microcins on the microbiota and impact of a high iron diet on microcin-mediated competition

a, High-iron diet design for **b–e** with SPF mice (n = 5/group) **b**, Ratio (EcN over cEc) in fecal content at days 1–5 post-intragastric inoculation. **c**, Cecal gene expression at day 5 post-inoculation (n = 3–4/group). **d,e**, CFU/mg of (d) cEc or (e) wild-type EcN or EcN *mchDEF* in indicated samples at days 1–5 post-inoculation when cEc was administered alone or in competition as indicated (n = 5/group). **f,g**, See Fig. 2a for experimental design with SPF mice. 16S ribosomal rRNA gene sequence analysis (V4 region) of fecal DNA obtained from mice pre-DSS administration (Day -4), post-DSS (Day 0), and day 5 post-intragastric inoculation of cEc with either wild-type EcN or EcN *mchDEF* at a 1:1 ratio. **f**, Eubacterial alpha diversity (inverse Simpson index); Shannon index yielded similar results. **g**, Principal coordinates (PCo) analysis plot (PCo1 vs. PCo2) of eubacterial beta diversity

Author Manuscript Author Manuscript Author Manuscript Author Manuscript

(weighted UniFrac); symbols as in panel **f. b,c,** Bars = geometric mean ± s.e.m. **d**,**e,f,g**, Individual symbol = mouse. **d,e**, bars = geometric mean. **f**, bars = mean ± s.d. n.s., not significant. Black symbols = comparisons within same day; red symbols = comparisons between days.

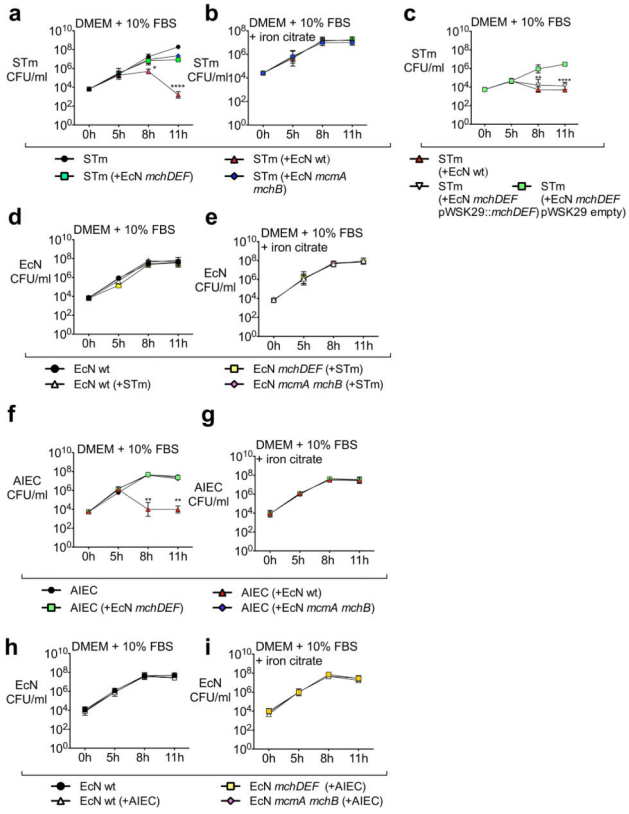

Extended Data Figure 6. *In vitro* activity of *E. coli* Nissle microcins against *S.* Typhimurium and AIEC

a–i, Strains were grown overnight in Nutrient Broth + 0.2 mM 2,2′-dipyridyl. Growth assays were performed in iron-limiting conditions (DMEM/F12 + 10% FBS) or in media supplemented with 1 μM iron citrate. Timepoints at 0, 5, 8 and 11 hours post-inoculation were collected. **a**,**b**, STm CFU/mL when grown alone or in competition with wild-type or mutant EcN in (**a**) iron-limiting conditions or in (**b**) media supplemented with 1 μM iron citrate. **c**, STm CFU/mL in iron-limiting conditions when in competition with wild-type EcN or an EcN *mchDEF* strain harboring either pWSK29::*mchDEF* or empty vector control. **d,e**, CFU/mL of wild-type or mutant EcN when grown alone or in competition with STm in (**d**) iron-limiting conditions or in (**e**) media supplemented with 1 μM iron citrate. **f**,**g**, AIEC CFU/mL when grown alone or in competition with wild-type or mutant EcN in (**f**) iron-limiting conditions or in (**g**) media supplemented with 1 μM iron citrate. **h**,**i**, CFU/mL of wild-type or mutant EcN when grown alone or in competition with AIEC in (**h**) iron-limiting conditions or in (**i**) media supplemented with 1 μM iron citrate. **a–i**, Symbols = geometric mean (three independent experiments) ± s.e.m. **P*<0.05, ***P*<0.01, ****P*<0.001, *****P*<0.0001.

Author Manuscript Author Manuscript Author Manuscript Author Manuscript

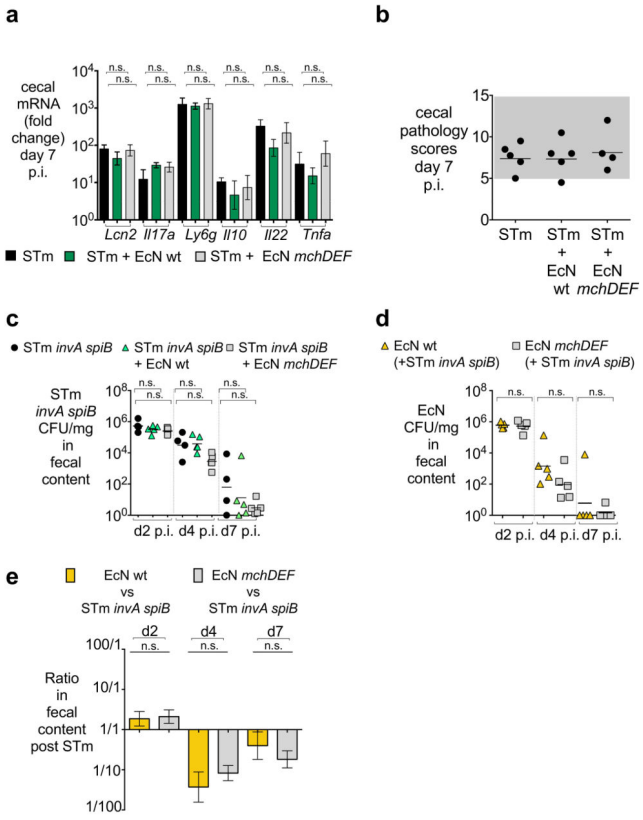

Extended Data Figure 7. Co-administration of *S.* Typhimurium with *E. coli* Nissle wild-type or EcN *mchDEF*

a–e, See Fig. 3d for co-administration design with SPF mice. **a,b**, Intragastric inoculation with wild-type STm. Cecal (**a**) gene expression (STm only, n = 7; all others, n = 9); data are expressed as fold change over mock-treated mice or (**b**) histopathology (STm only and STm + wild-type EcN, n = 5; STm + EcN *mchDEF*, n = 4) from mice shown in Fig. 3f,g at Day 7 post-infection. **c–e**, Intragastric inoculation with STm *invA spiB*. **c,d**, CFU/mg of (**c**) STm *invA spiB* (n = 4) or (**d**) wild-type EcN or EcN *mchDEF* in fecal content at designated timepoints post-infection when STm *invA spiB* was administered alone or in competition as indicated (n = 5/group). **e**, Ratio of wild-type EcN or EcN *mchDEF* over STm *invA spiB* in fecal content at designated timepoints post-infection (n = 5/group). **a,e,** Bars = geometric mean ± s.e.m. **b–d**, Individual symbol = mouse. **b**, Bars = mean. **c,d**, Bars = geometric mean. n.s., not significant.

Author Manuscript Author Manuscript Author Manuscript Author Manuscript

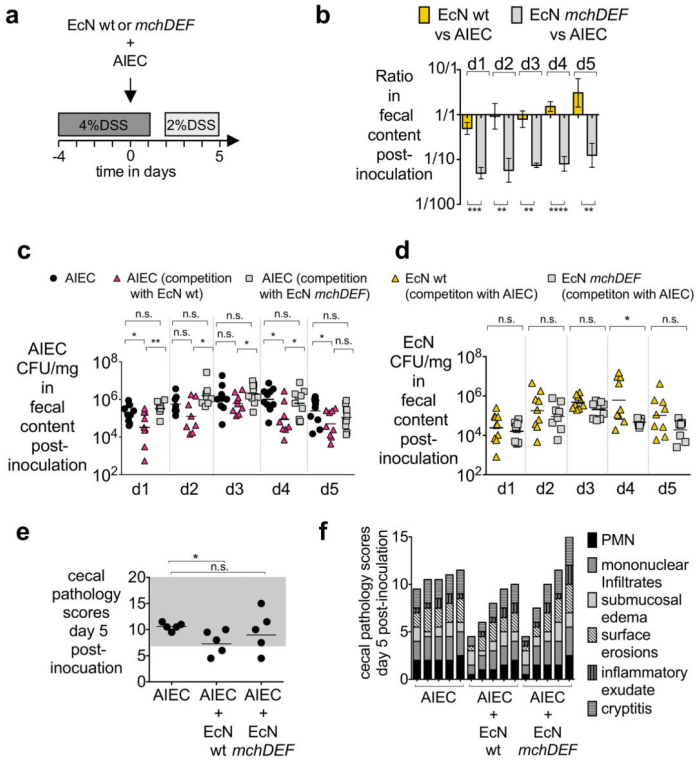

Extended Data Figure 8. Gut colonization of AIEC in DSS-treated mice when competing with *E. coli* Nissle wild-type or EcN *mchDEF*

a, Experimental design for **b–f** with SPF mice. **b,** Ratio of wild-type EcN or EcN *mchDEF* over AIEC in fecal content at days 1–5 post-intragastric inoculation (n = 9/group). Bars = geometric mean ± s.e.m. **c,d**, CFU/mg of (**c**) AIEC or (**d**) wild-type EcN or EcN *mchDEF* in fecal content at days 1–5 post-inoculation when AIEC was administered alone or in competition as indicated (n = 9/group). **e**, Cecal histopathology scores at day 5 post-inoculation for panels **c,d** (n = 5/group). **f**, Detailed histopathology scoring of panel **e** mice. **b**, Bars = geometric mean ± s.e.m. **c–e**, Individual symbol = mouse. **c,d**, Bars = geometric mean. **e**, Bars = mean. **P*<0.05, ***P*<0.01, ****P*<0.001, *****P*<0.0001; n.s., not significant.

Author Manuscript Author Manuscript Author Manuscript Author Manuscript

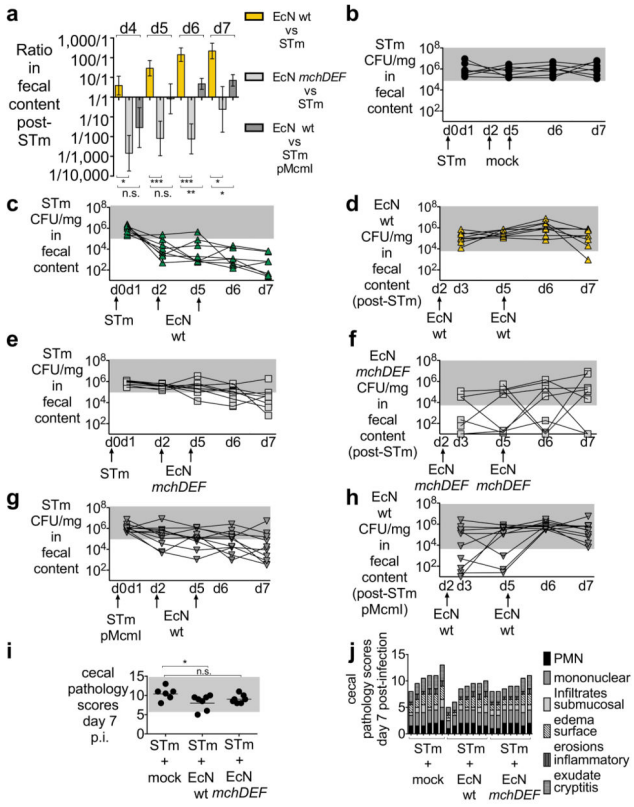

Extended Data Figure 9. Therapeutic administration of *E. coli* Nissle wild-type, EcN *mchDEF* or mock during *S.* Typhimurium infection

a–j, See Fig. 4a for therapeutic design with SPF mice. **a–f**, Intragastric inoculation with wild-type STm. **a,** Ratio of wild-type EcN or EcN *mchDEF* over STm in fecal content on days 4–7 post-infection with STm (n = 8/group). **b**,**c**,**e**, STm CFU/mg at designated timepoints post-infection in fecal content of mice therapeutically treated with (**b**) mock (n = 7), (**c**) wild-type EcN (n = 8) or (**e**) EcN *mchDEF* (n = 8). **d**,**f**, CFU/mg of (**d**) wild-type EcN or (**f**) EcN *mchDEF* in fecal content at designated timepoints post-STm infection. **g,h**, Intragastric inoculation with STm pMcmI (n = 10/group). CFU/mg of (**g**) STm pMcmI or (**h**) wild-type EcN in fecal content at designated timepoints post-STm pMcmI infection. Grey box represents average STm CFU/mg in mock-treated mice (panel **b**). **i**, Cecal histopathology scores for panels **b–f** (STm alone, n = 6; all others, n = 7). **j**, Detailed histopathology scoring of panel **i** mice. **a**, Bars = geometric mean ± s.e.m. **i**, Bars = mean. **P*< 0.05, ***P*< 0.01, ****P*< 0.001; n.s., not significant.

Author Manuscript Author Manuscript Author Manuscript Author Manuscript

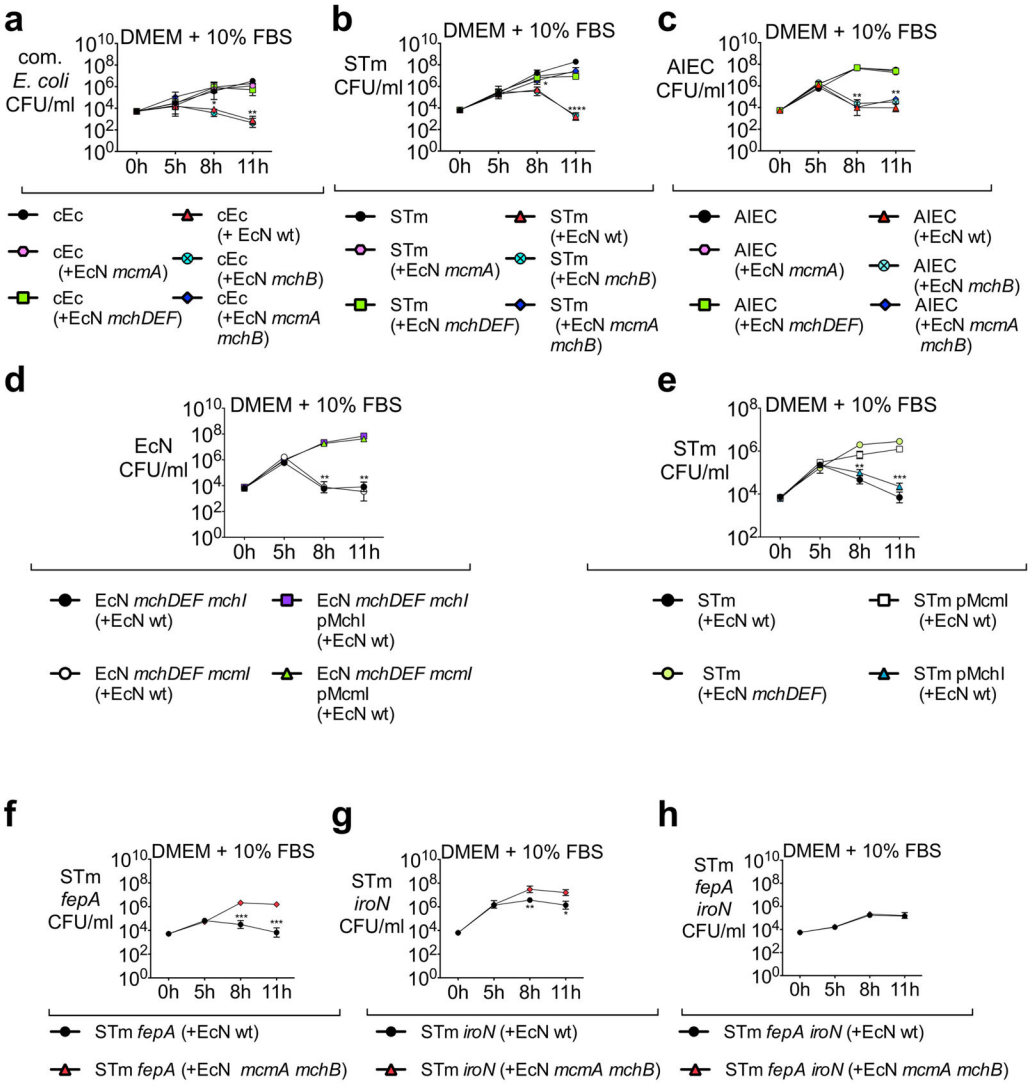

Extended Data Figure 10. *In vitro* growth curves of microcin M (*mcmA*) and microcin H47 (*mchB*) EcN mutants in competition with commensal *E. coli*, *S.* Typhimurium, or AIEC

a–h, Strains were grown overnight in Nutrient Broth + 0.2 mM 2,2′-dipyridyl. Growth assays were performed in iron-limiting conditions (DMEM/F12 + 10% FBS) and timepoints at 0, 5, 8 and 11 hours post-inoculation were collected. **a–c**, CFU/mL of (**a**) commensal *E. coli*, (**b**) STm or (**c**) AIEC when grown alone or in competition with the indicated EcN strain. **d**, CFU/mL of complemented and uncomplemented EcN microcin immunity gene mutants when in competition with EcN wild-type. **e**, CFU/mL of wild-type STm or STm harboring pMchI or pMcmI when in competition with EcN wild-type. **f-h**, CFU/mL of (**f**) STm *fepA*, (**g**) STm *iroN* and (**h**) STm *fepA iroN* in competition with either wild-type EcN or EcN *mcmA mchB*. **a–h**, Symbols = geometric mean (three independent experiments) ± s.e.m. **P*< 0.05, ***P*< 0.01, ****P*< 0.001, *****P*< 0.0001.

Author Manuscript Author Manuscript Author Manuscript Author Manuscript

Supplementary Material

Refer to Web version on PubMed Central for supplementary material.

Acknowledgments

We would like to acknowledge Dr. Elizabeth Nolan for critically reading our manuscript, Dr. Judith Behnsen for setting up the Raffatellu lab germ-free mouse facility, and Dr. Maria Valeri, Dr. Araceli Perez-Lopez, Dr. Vladimir Diaz-Ochoa, and Evelyn Hoover for contributing to the maintenance of the germ-free facility. We would also like to thank Dr. Wenhan Zhu and Dr. Sebastian Winter for providing us with the protocol for cleaning up DNA stool samples from DSS, and Matthew Rolston at the UC Davis Host-Microbe Systems Biology Core for processing samples for Illumina MiSeq Analysis. We would like to acknowledge the students of the 2015 Summer course "Frontiers in Host-Microbe Interactions", Marine Biology Laboratory, who helped with the generation of one dataset for the manuscript. Work in Manuela Raffatellu's lab is supported by Public Health Service Grants AI083663, AI126277, AI101784, AI114625, AI105374, and DK058057. Manuela Raffatellu holds an Investigator in the Pathogenesis of Infectious Disease Award from the Burroughs Wellcome Fund.

References

1. Donaldson GP, Lee SM, Mazmanian SK. Gut biogeography of the bacterial microbiota. Nat Rev Microbiol. 2016; 14:20–32. [PubMed: 26499895]
2. Winter SE, Bäumler AJ. Why related bacterial species bloom simultaneously in the gut: principles underlying the 'Like will to like' concept. Cell Microbiol. 2014; 16:179–184. [PubMed: 24286560]
3. Stecher B. The Roles of Inflammation, Nutrient Availability and the Commensal Microbiota in Enteric Pathogen Infection. Microbiol Spectr. 2015; 3
4. Ng KM, et al. Microbiota-liberated host sugars facilitate post-antibiotic expansion of enteric pathogens. Nature. 2013; 502:96–99. [PubMed: 23995682]
5. Winter SE, et al. Host-derived nitrate boosts growth of *E coli* in the inflamed gut. Science. 2013; 339:708–711. [PubMed: 23393266]
6. Winter SE, Lopez CA, Bäumler AJ. The dynamics of gut-associated microbial communities during inflammation. EMBO Rep. 2013; 14:319–327. [PubMed: 23478337]
7. Rebuffat S. Microcins in action: amazing defence strategies of Enterobacteria. Biochem Soc Trans. 2012; 40:1456–1462. [PubMed: 23176498]
8. Yang SC, Lin CH, Sung CT, Fang JY. Antibacterial activities of bacteriocins: application in foods and pharmaceuticals. Front Microbiol. 2014; 5:241. [PubMed: 24904554]
9. Kamada N, Chen GY, Inohara N, Nuñez G. Control of pathogens and pathobionts by the gut microbiota. Nat Immunol. 2013; 14:685–690. [PubMed: 23778796]
10. Buffie CG, Pamer EG. Microbiota-mediated colonization resistance against intestinal pathogens. Nat Rev Immunol. 2013; 13:790–801. [PubMed: 24096337]
11. Baquero FFM. The microcins. FEMS Microbiology Letters. 1978; 23:117–124.
12. Behnsen J, Deriu E, Sassone-Corsi M, Raffatellu M. Probiotics: properties, examples, and specific applications. Cold Spring Harb Perspect Med. 2013; 3:10074.
13. Jacobi CA, Malfertheiner P. *Escherichia coli* Nissle 1917 (Mutaflor): new insights into an old probiotic bacterium. Dig Dis. 2011; 29:600–607. [PubMed: 22179217]
14. Patzer SI, Baquero MR, Bravo D, Moreno F, Hantke K. The colicin G, H and X determinants encode microcins M and H47, which might utilize the catecholate siderophore receptors FepA, Cir, Fiu and IroN. Microbiology. 2003; 149:2557–2570. [PubMed: 12949180]
15. Kommineni S, et al. Bacteriocin production augments niche competition by enterococci in the mammalian gastrointestinal tract. Nature. 2015; 526:719–722. [PubMed: 26479034]
16. Nolan EM, Walsh CT. Investigations of the MceIJ-catalyzed posttranslational modification of the microcin E492 C-terminus: linkage of ribosomal and nonribosomal peptides to form "trojan horse" antibiotics. Biochemistry. 2008; 47:9289–9299. [PubMed: 18690711]
17. Sassone-Corsi M, Raffatellu M. No vacancy: how beneficial microbes cooperate with immunity to provide colonization resistance to pathogens. J Immunol. 2015; 194:4081–4087. [PubMed: 25888704]

Author Manuscript Author Manuscript Author Manuscript Author Manuscript

18. Behnsen J, et al. The cytokine IL-22 promotes pathogen colonization by suppressing related commensal bacteria. Immunity. 2014; 40:262–273. [PubMed: 24508234]
19. Duquesne S, Destoumieux-Garzon D, Peduzzi J, Rebuffat S. Microcins, gene-encoded antibacterial peptides from enterobacteria. Nat Prod Rep. 2007; 24:708–734. [PubMed: 17653356]
20. Rebuffat S, Blond A, Destoumieux-Garzon D, Goulard C, Peduzzi J. Microcin J25, from the macrocyclic to the lasso structure: implications for biosynthetic, evolutionary and biotechnological perspectives. Curr Protein Pept Sci. 2004; 5:383–391. [PubMed: 15544533]
21. Vassiliadis G, Destoumieux-Garzon D, Lombard C, Rebuffat S, Peduzzi J. Isolation and characterization of two members of the siderophore-microcin family, microcins M and H47. Antimicrob Agents Chemother. 2010; 54:288–297. [PubMed: 19884380]
22. Fischbach MA, Lin H, Liu DR, Walsh CT. How pathogenic bacteria evade mammalian sabotage in the battle for iron. Nat Chem Biol. 2006; 2:132–138. [PubMed: 16485005]
23. Deriu E, et al. Probiotic bacteria reduce *Salmonella* Typhimurium intestinal colonization by competing for iron. Cell Host Microbe. 2013; 14:26–37. [PubMed: 23870311]
24. Raffatellu M, et al. Lipocalin-2 resistance confers an advantage to *Salmonella* enterica serotype Typhimurium for growth and survival in the inflamed intestine. Cell Host Microbe. 2009; 5:476–486. [PubMed: 19454351]
25. Zheng T, Nolan EM. Enterobactin-mediated delivery of beta-lactam antibiotics enhances antibacterial activity against pathogenic *Escherichia coli*. Journal of the American Chemical Society. 2014; 136:9677–9691. [PubMed: 24927110]
26. Eaves-Pyles T, et al. Escherichia coli isolated from a Crohn's disease patient adheres, invades, and induces inflammatory responses in polarized intestinal epithelial cells. Int J Med Microbiol. 2008; 298:397–409. [PubMed: 17900983]
27. Datsenko KA, Wanner BL. One-step inactivation of chromosomal genes in *Escherichia coli* K-12 using PCR products. Proc Natl Acad Sci USA. 2000; 97:6640–6645. [PubMed: 10829079]
28. Caporaso JG, et al. QIIME allows analysis of high-throughput community sequencing data. Nature methods. 2010; 7:335–336. [PubMed: 20383131]

Author Manuscript Author Manuscript Author Manuscript Author Manuscript

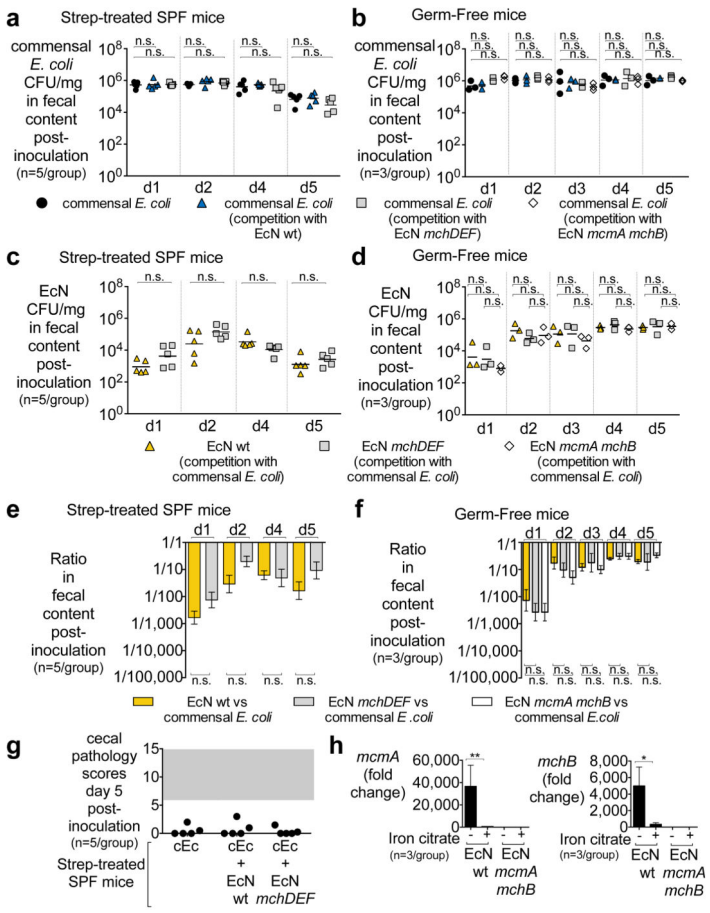

Figure 1. Microcins do not promote bacterial competition in the absence of intestinal inflammation

a,**c**,**e**,**g**, SPF streptomycin-treated (day -1) mice or **b**,**d**,**f**, germ-free mice were intragastrically inoculated with indicated *E. coli* strain(s). **a**–**d**, CFU/mg feces from (**a**,**c**) SPF or (**c**,**d**) germ-free mice on days 1–5 post-inoculation. **e**,**f**, Ratio (EcN over commensal) of (**e**) panels **a**,**c** or (**f**) panels **b**,**d**; bars = mean ± s.e.m. **g**, Cecal histopathology scores for panels **a**,**c** mice. **a**–**d**,**g**, Symbol = individual mouse; bars = geometric mean. **h**, *gapA*-normalized *mcmA* (microcin M) and *mchB* (microcin H47) mRNA levels in iron-rich and iron-limited media. Bars = geometric mean (three independent experiments) ± s.e.m. **P*<0.05, ***P*<0.01; n.s., not significant. Unpaired Student's *t* test was utilized for statistical comparisons in panel **h**, Mann-Whitney-Wilcoxon for all other comparisons; *P*-values are presented in Supplementary Table 7.

Author Manuscript Author Manuscript Author Manuscript Author Manuscript

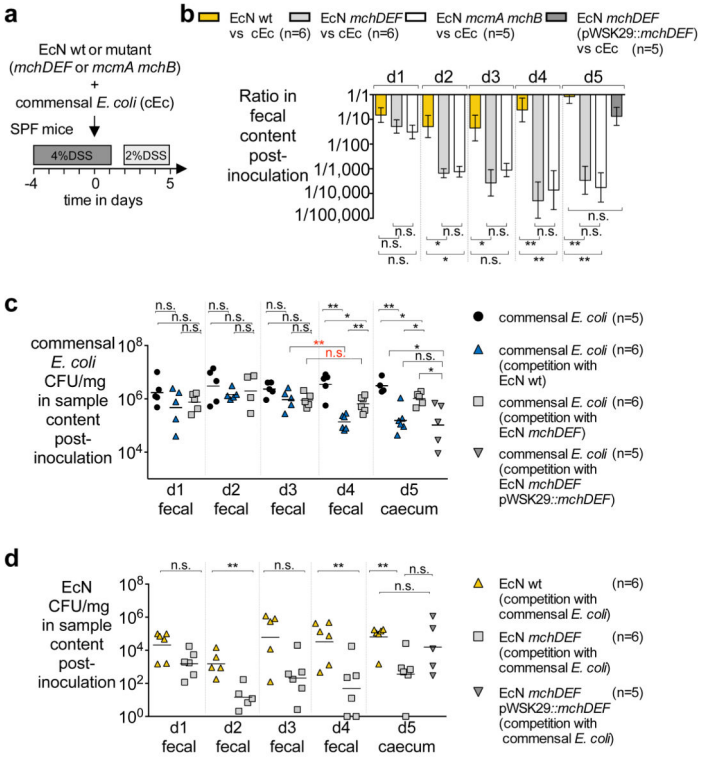

Figure 2. Microcins enable *E. coli* Nissle to limit the expansion of a commensal *E. coli* in the inflamed gut

a, Experimental design for **b**–**d. b**–**d**, (**b**) Ratio (EcN over commensal) or (**c**,**d**) CFU/mg sample at days 1–5 post-intragastric inoculation of indicated *E. coli* strain(s). **b**, Bars = mean ± s.e.m. **c**,**d**, Symbol = individual mouse; bars = geometric mean; data represent two experiments. **P*<0.05, ***P*<0.01; n.s., not significant. Statistics in black compare same timepoint; red compare different timepoints. Mann-Whitney-Wilcoxon was utilized for all statistical comparisons; *P*-values are presented in Supplementary Table 7.

Author Manuscript Author Manuscript Author Manuscript Author Manuscript

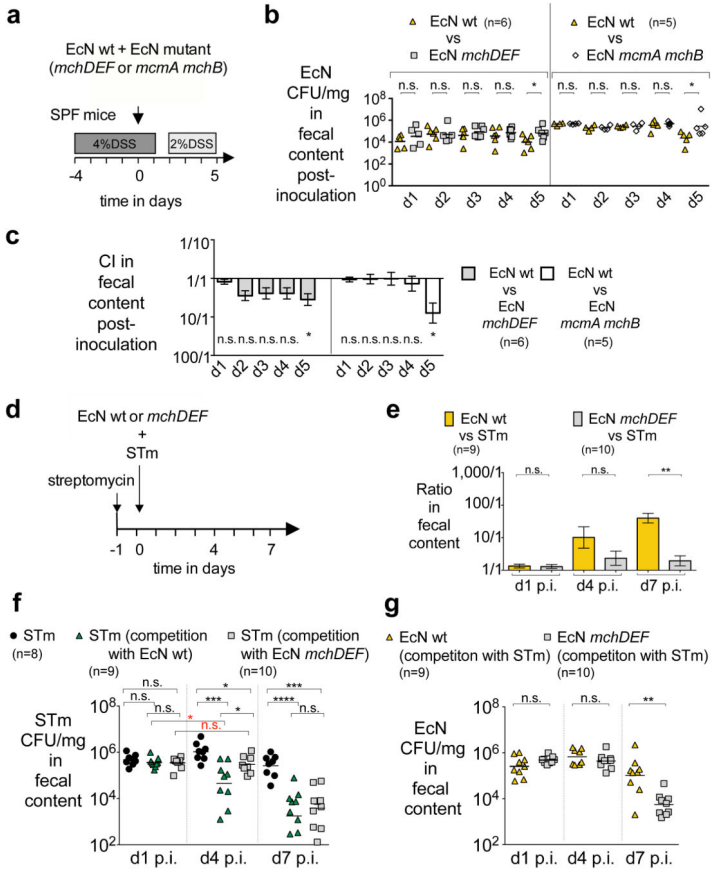

Figure 3. *E. coli* Nissle utilizes microcins to outcompete an enteric pathogen when the strains are co-administered

a, Experimental design for **b**,**c. b**,**c**, (**b**) CFU/mg feces or (**c**) competitive index (CI; EcN wild-type over mutant) at days 1–5 post-intragastric inoculation of indicated *E. coli* strains. **d**, Co-administration design for **e**-**g. e**–**g,** (**e**) Ratio (EcN over STm) or (**f**,**g**) CFU/mg feces at designated timepoints post-intragastric inoculation of indicated strain(s). **c**,**e**, Bars = mean ± s.e.m. **b**,**f**,**g**, symbol = mouse; bars = geometric mean; data represent 2 independent experiments. **P*<0.05, ***P*<0.01, ****P*<0.001, *****P*<0.0001; n.s., not significant. Statistics in black compare same timepoint; red compares different timepoints. Mann-Whitney-Wilcoxon was utilized for all statistical comparisons; *P*-values are presented in Supplementary Table 7.

Author Manuscript Author Manuscript Author Manuscript Author Manuscript

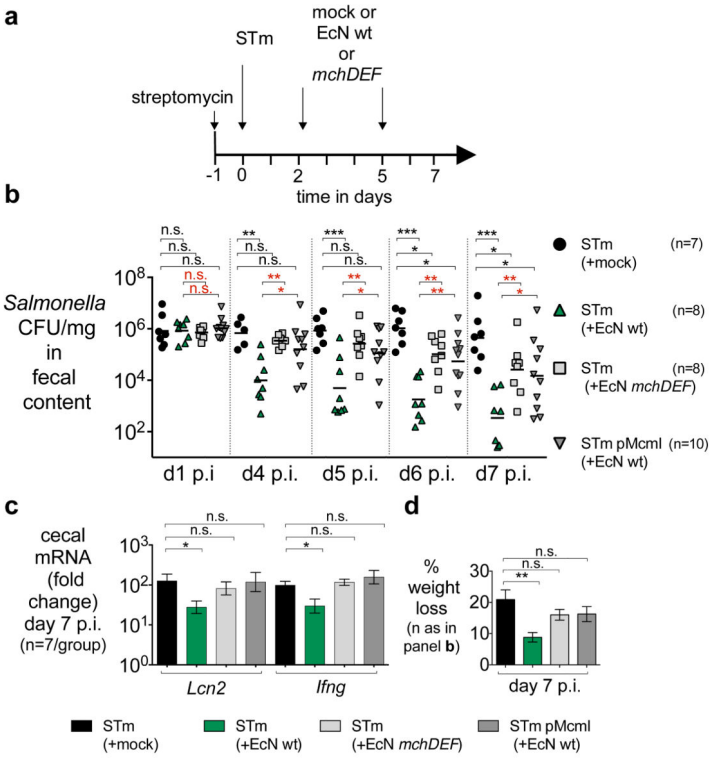

Figure 4. Microcins therapeutically reduce colonization of an enteric pathogen in the inflamed gut

a, Therapeutic design for **b–d** and Extended Data Fig. 9. b, *Salmonella* CFU/mg feces, days 1 and 4–7 post-infection. For panel **b** mice, day 7: **c**, cecal mRNA levels; **d**, weight loss. **b**, symbol = mouse; bars = geometric mean; data represent 2 independent experiments. **c**,**d**, Bars = mean ± s.e.m. **P*<0.05, ***P*<0.01, ****P*<0.001; n.s., not significant. Statistics in black compare to STm (+mock); red compares to STm (+EcN wt). Mann-Whitney-Wilcoxon was utilized for all statistical comparisons; *P*-values are presented in Supplementary Table 7.